nature nanotechnology
SUPPLEMENTARY INFORMATION
DOI: 10.1038/NNANO.2015.186

Dielectric metasurfaces for complete control of phase and polarization with subwavelength spatial resolution and high transmission

Amir Arbabi, Yu Horie, Mahmood Bagheri, and Andrei Faraon

DOI: 10.1038/NNANO.2015.186

S1. ARBITRARY POLARIZATION AND PHASE TRANSFORMATION USING SYMMETRIC AND UNITARY JONES MATRICES

Here we show that any arbitrary polarization and phase transformation can always be performed using a unitary and symmetric Jones matrix. We prove this by determining the unitary and symmetric Jones matrix $\mathbf{T}$ that maps a given input electric field $\mathbf{E}^{\text{in}}$ to a desired output electric field $\mathbf{E}^{\text{out}}$. For polarization and phase transformations (i.e. no amplitude modification), the Jones matrix should be unitary since the transmitted power is equal to the incident power and $|\mathbf{E}^{\text{out}}| = |\mathbf{E}^{\text{in}}|$. The general relation between the electric fields of input and output optical waves for normal incidence is expressed as $\mathbf{E}^{\text{out}} = \mathbf{T}\mathbf{E}^{\text{in}}$. For a symmetric and unitary Jones matrix we have

$$T_{xx}E_x^{\text{in}} + T_{yx}E_y^{\text{in}} = E_x^{\text{out}}, \tag{1a}$$

$$T_{yx}E_x^{\text{in}} - \frac{T_{yx}}{T_{yx}{}^*}T_{xx}{}^*E_y^{\text{in}} = E_y^{\text{out}}, \tag{1b}$$

where E_x^{in} and E_y^{in} are the x and y components of the electric field of the input light, E_x^{out} and E_y^{out} are the x and y components of the electric field of the output light, T_{ij} $(i, j = x, y)$ are the elements of the 2×2 Jones matrix, and * represents complex conjugation. In deriving Eqs. 1a and 1b, we have used the symmetric properties $T_{xy} = T_{yx}$, and the unitary condition $T_{xx}T_{xy}{}^* + T_{yx}{}^*T_{yy} = 0$. By multiplying Eq. 1a by $T_{xx}{}^*$ and Eq. 1b by $T_{yx}{}^*$ we obtain

$$|T_{xx}|^2E_x^{\text{in}} + T_{yx}T_{xx}{}^*E_y^{\text{in}} = T_{xx}{}^*E_x^{\text{out}}, \tag{2a}$$

$$|T_{yx}|^2E_x^{\text{in}} - T_{yx}T_{xx}{}^*E_y^{\text{in}} = T_{yx}{}^*E_y^{\text{out}}. \tag{2b}$$

By adding Eqs. 2a and 2b, using the unitary condition $|T_{xx}|^2 + |T_{yx}|^2 = 1$, and taking the complex conjugate of the resultant relation, we find

$$T_{xx}E_x^{\text{out}*} + T_{yx}E_y^{\text{out}*} = E_x^{\text{in}*}. \tag{3}$$

Finally, by expressing Eqs. 3 and 1a in the matrix form, we obtain

$$\begin{bmatrix} E_x^{\text{out}*} & E_y^{\text{out}*} \\ E_x^{\text{in}} & E_y^{\text{in}} \end{bmatrix} \begin{bmatrix} T_{xx} \\ T_{yx} \end{bmatrix} = \begin{bmatrix} E_x^{\text{in}*} \\ E_x^{\text{out}} \end{bmatrix}. \tag{4}$$

Therefore, for any given $\mathbf{E}^{\text{in}}$ and $\mathbf{E}^{\text{out}}$, we can find T_{xx} and T_{yx} from Eq. 4, and T_{xy} and T_{yy} from the symmetry and unitary conditions as

$$T_{xy} = T_{yx}, \tag{5a}$$

$$T_{yy} = -\exp(2i\angle T_{yx}){T_{xx}}^*. \tag{5b}$$

Thus, we can always find a unitary and symmetric Jones matrix that transforms any input optical wave $\mathbf{E}^{\text{in}}$ to any output optical wave $\mathbf{E}^{\text{out}}$.

S2. REALIZATION OF ANY SYMMETRIC AND UNITARY JONES MATRICES USING A UNIFORM BIREFRINGENT METASURFACE

Here we show that any symmetric and unitary Jones matrix can be realized using a uniform birefringent metasurface shown in Fig. 2a in the main text, if ϕ_x, ϕ_y, and the angle between one of the principal axis of the metasurface and the x axis (θ) could be chosen freely. Any symmetric and unitary matrix is decomposable in terms of its eigenvectors and eigenvalue matrix ($\mathbf{\Delta}$) as

$$\mathbf{T} = \mathbf{V}\begin{bmatrix} \mathrm{e}^{i\phi_x} & 0 \\ 0 & \mathrm{e}^{i\phi_y} \end{bmatrix}\mathbf{V}^T = \mathbf{R}(\theta)\mathbf{\Delta}\mathbf{R}(-\theta), \tag{6}$$

where superscript T represents the matrix transpose operation. $\mathbf{V}$ is a real unitary matrix; therefore, it corresponds to an in-plane geometrical rotation $\mathbf{R}$ by an angle that we refer to as θ, and since $\mathbf{V}^T = \mathbf{V}^{-1}$, $\mathbf{V}^T$ represents a rotation by $-\theta$. According to Eq. 6, the operation of a metasurface that realizes the Jones matrix $\mathbf{T}$ can be considered as rotating the electric field of the input wave ($\mathbf{E}^{\text{in}}$) by $-\theta$, phase shifting the x and y components of the rotated $\mathbf{E}^{\text{in}}$ respectively by ϕ_x and ϕ_y, and rotating back the rotated and phase shifted vector by angle θ. Equivalently, $\mathbf{T}$ can be implemented using a metasurface that imposes phase shifts ϕ_x and ϕ_y to the components of $\mathbf{E}^{\text{in}}$ along angles θ and $90°+\theta$, respectively. Such a metasurface is realized by starting with a metasurface whose principal axis are along x and y directions and imparts ϕ_x and ϕ_y phase shifts to x and y-polarized waves, and rotating it anticlockwise by angle θ. Therefore, any symmetric and unitary Jones matrix can be realized using a metasurface if its ϕ_x, ϕ_y, and in-plane rotation angle (θ) could be chosen freely.

 DOI: 10.1038/NNANO.2015.186

S3. INDEPENDENT WAVEFRONT CONTROL FOR TWO ORTHOGONAL POLARIZATIONS

In this section, we derive the necessary condition for the design of a device that imposes two independent phase profiles to two optical waves with orthogonal polarizations. The four elements of the Jones matrix $\mathbf{T}$ are found uniquely using Eqs. 4 and 5, when the determinant of the matrix on the left hand side of Eq. 4 is nonzero. Therefore, a devices that is designed to map $\mathbf{E}^{\mathrm{in}}$ to $\mathbf{E}^{\mathrm{out}}$, converts an optical wave whose polarization is orthogonal to $\mathbf{E}^{\mathrm{in}}$ to an optical wave polarized orthogonal to $\mathbf{E}^{\mathrm{out}}$. For example, an optical element designed to generate radially polarized light from x polarized input light, will also generate azimuthally polarized light from y polarized input light.

In the special case that the determinant of the matrix on the left had side of Eq. 4 is zero we have

$$E_x^{\mathrm{out}*}E_y^{\mathrm{in}} - E_y^{\mathrm{out}*}E_x^{\mathrm{in}} = 0, \tag{7}$$

and because $\mathbf{T}$ is unitary we have $|\mathbf{E}^{\mathrm{in}}| = |\mathbf{E}^{\mathrm{out}}|$; therefore we find $\mathbf{E}^{\mathrm{out}} = \exp(i\phi)\mathbf{E}^{\mathrm{in}*}$ where ϕ is an arbitrary phase. This special case corresponds to a device that preserves the polarization ellipse of the input light, switches its handedness (helicity), and imposes a phase shift on it. In this case, the $\mathbf{T}$ matrix is not uniquely determined from Eq. 4, and an additional condition, such as the phase profile for the orthogonal polarization, can be imposed on the operation of the device. Therefore, the device can be designed to realize two different phase profiles for two orthogonal input polarizations.

SUPPLEMENTARY VIDEO LEGENDS

Supplementary Video 1| Polarization switchable phase hologram. Movie showing the evolution of the image generated by a polarization switchable hologram as the polarization direction (shown by an arrow on the bottom left) of the illumination light is changed.

SUPPLEMENTARY FIGURES

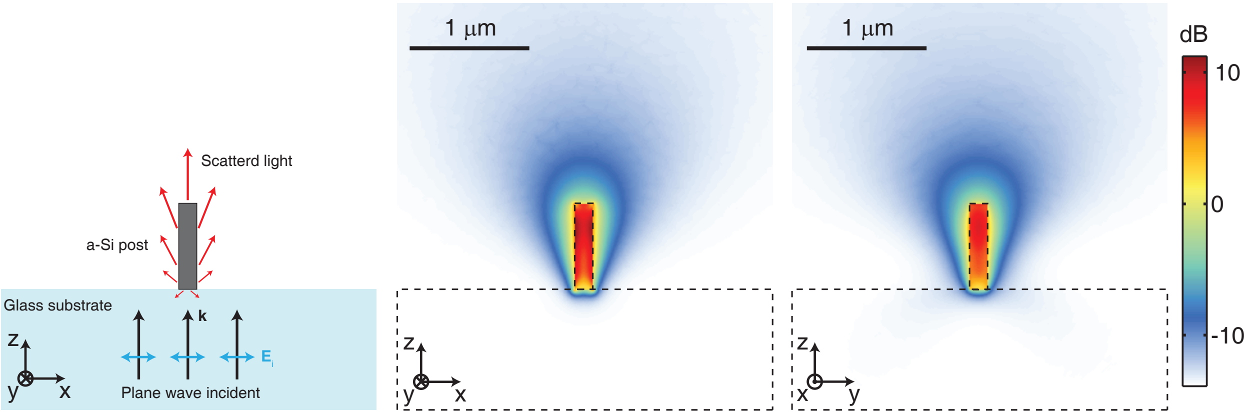

Supplementary Fig. 1. **Large forward scattering by a single amorphous silicon post**. Schematic illustration and finite element simulation results of light scattering by a single 715 nm tall circular amorphous silicon post with a diameter of 150 nm. The simulation results show the logarithmic scale energy density of the light scattered by the single amorphous silicon post over the xz and yz planes. The energy densities are normalized to the energy density of the 915 nm x-polarized incident plane wave.

 DOI: 10.1038/NNANO.2015.186

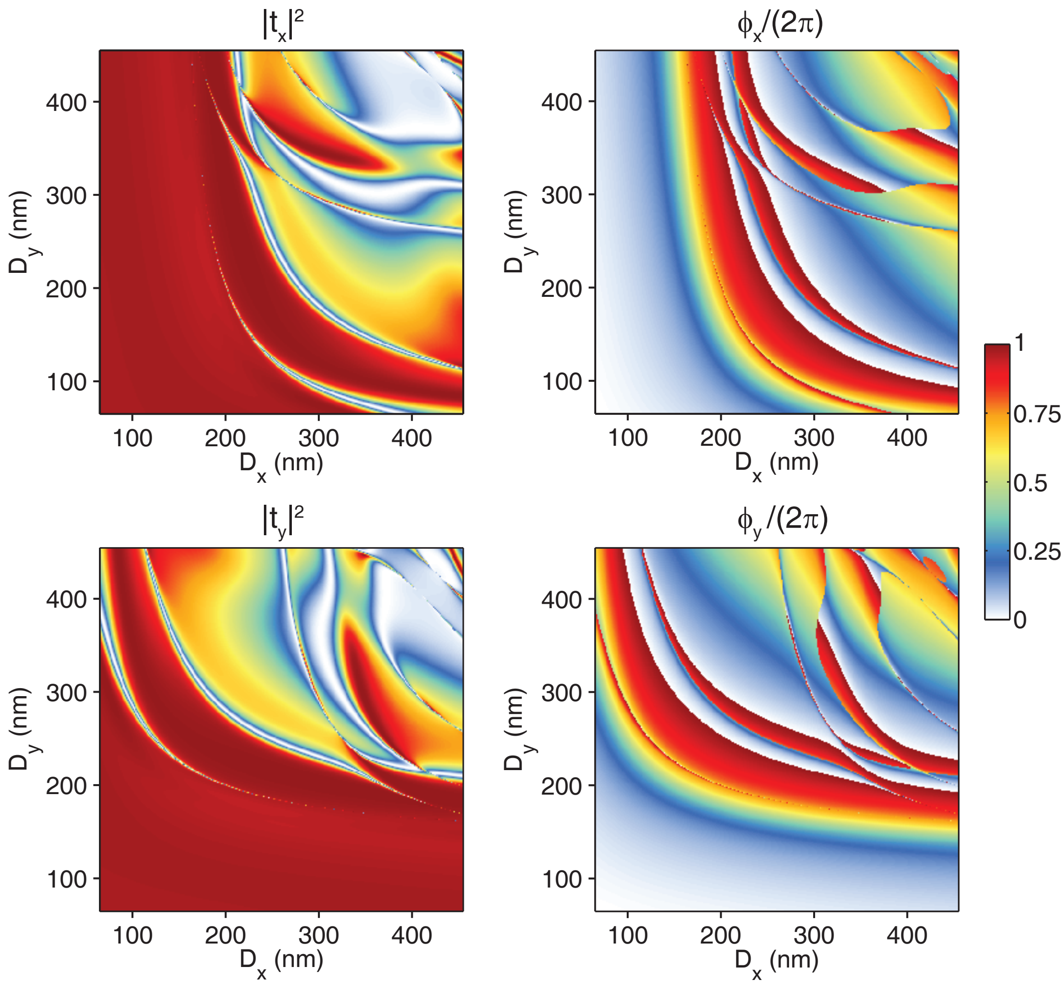

Supplementary Fig. 2. Phase shifts and intensity transmission coefficients as a function of elliptical post diameters, used to derive data in Fig. 2b-e of the main text. Intensity transmission coefficients ($|t_x|^2$ and $|t_y|^2$) and the phase of transmission coefficients (ϕ_x and ϕ_y) of x and y-polarized optical waves for the periodic array of elliptical posts shown in Fig. 2a of the main text as functions of the post diameters.

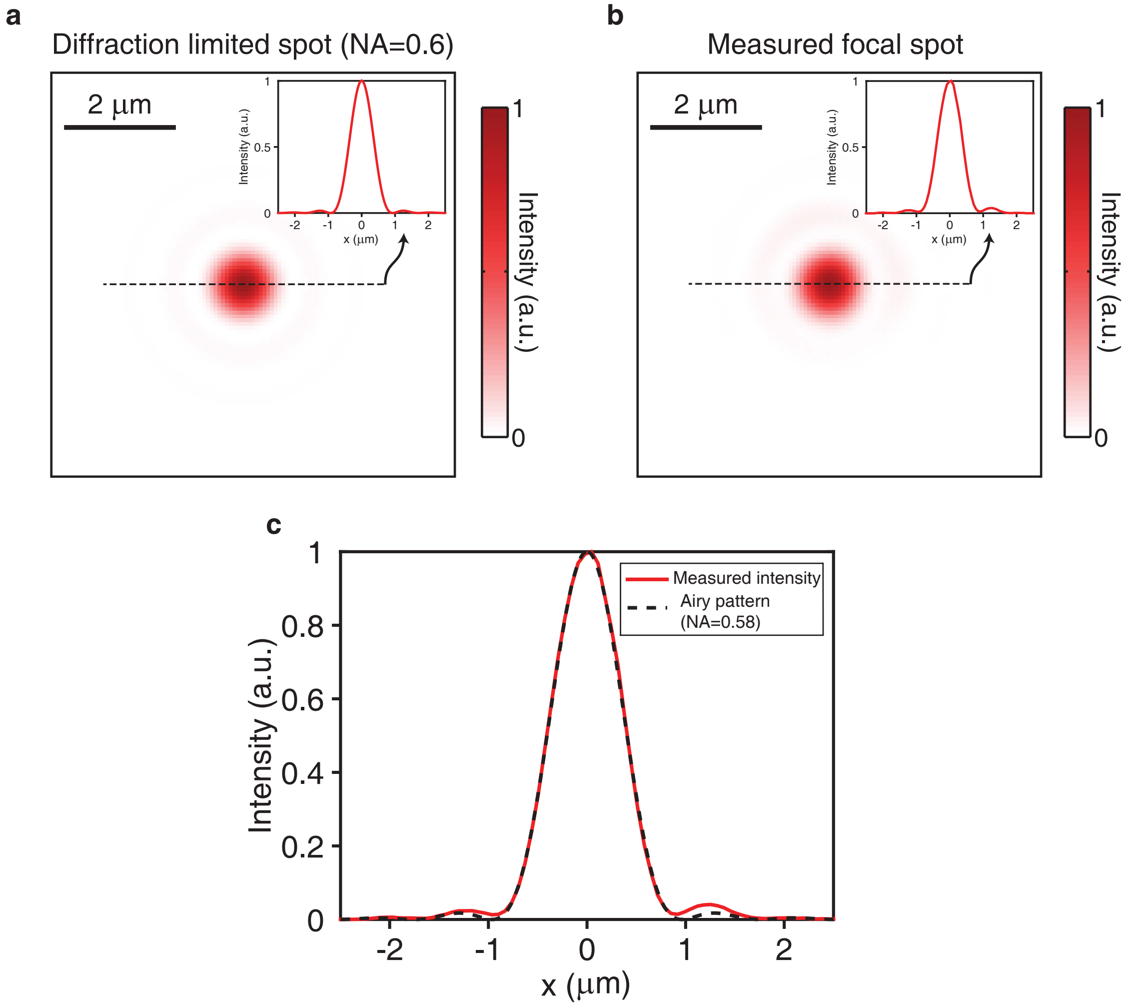

Supplementary Fig. 3. **Diffraction limited focusing by device shown in Fig. 5c**. **a**, Theoretical diffraction limited focal spot (Airy disk) for a lens with numerical aperture (NA) of 0.6 at the operation wavelength of 915 nm. Inset shows the intensity along the dashed line.**b**, Measured focal spot for the device shown in Fig. 5c when the device is uniformly illuminated with right handed circularly polarized 915 nm light. Inset shows the intensity along the dashed line. **c**, Measured intensity along the dashed line shown in (**b**) and its least squares Airy pattern fit which has an NA of 0.58.

 DOI: 10.1038/NNANO.2015.186

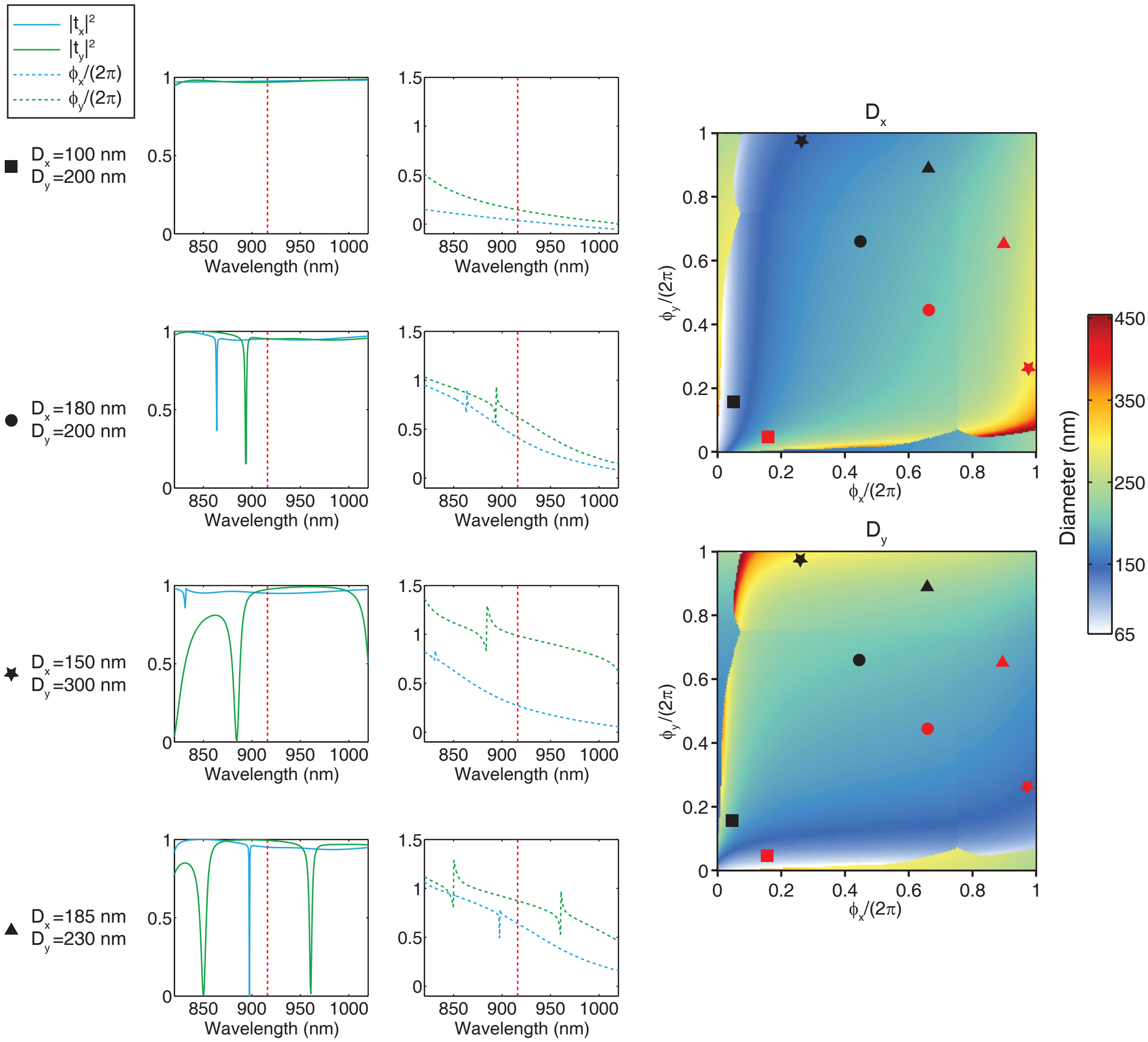

Supplementary Fig. 4. **Transmission spectra of periodic arrays of elliptical posts showing that the operation wavelength does not overlap with resonances**. Wavelength dependence of the intensity transmission coefficients ($|t_x|^2$ and $|t_y|^2$) and the phase of transmission coefficients (ϕ_x and ϕ_y) of x and y-polarized optical waves for the periodic arrays schematically shown in Fig. 2a of the main text. The spectra are shown for a few arrays with different (D_x, D_y) combinations: (100 nm, 200 nm), (180 nm, 200 nm), (150 nm, 300 nm), (185 nm, 230 nm). The corresponding phase shift values and post diameters for these arrays are shown on the D_x and D_y graphs on the right with black symbols. For brevity, only the spectra for the arrays with $D_y > D_x$ are shown. The transmission and phase spectra for the arrays with $D_x > D_y$ (which are shown with red symbols on the D_x and D_y graphs) can be obtained by swapping x and y in the spectra graphs. The desired operation wavelength (λ =915 nm) is shown with dashed red vertical lines in the spectra plots, and it does not overlap with any of the resonances of the periodic arrays.

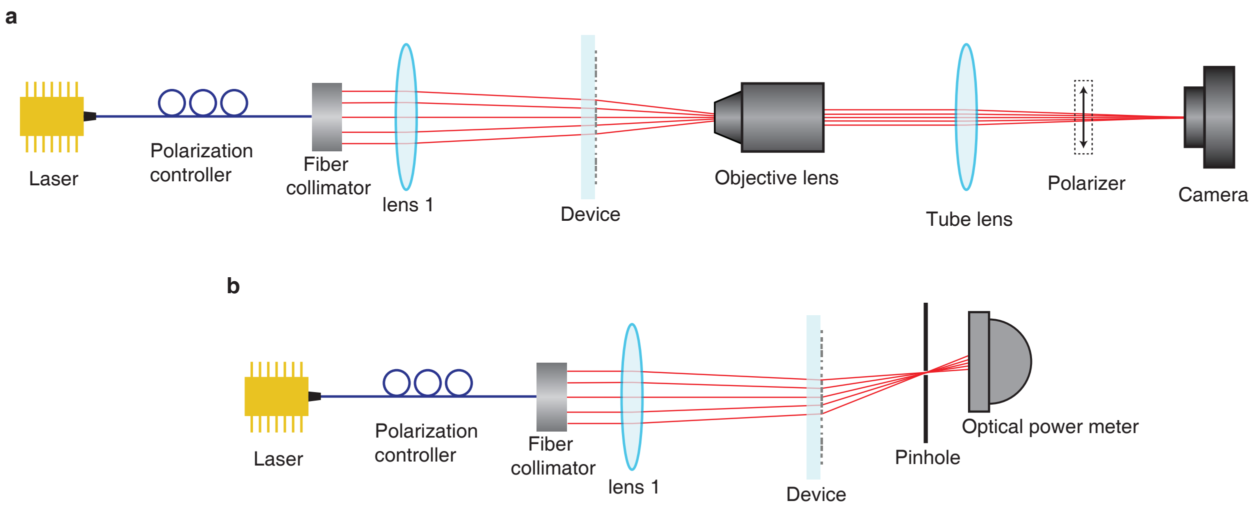

Supplementary Fig. 5. **Measurement setup**. **a**, Schematic illustration of the measurement setup used for characterization of devices modifying polarization and phase of light. The linear polarizer was inserted into the setup only during the polarization measurements. **b**, Schematic drawing of the experimental setup used for efficiency characterization of the device shown in Fig. 4b.